

Design calculations for fast plasma position control in Korea Superconducting Tokamak Advanced Research

Hogun Jhang ^{a,*}, C. Kessel ^b, N. Pomphrey ^b, S.C. Jardin ^b, G.S. Lee ^a,
C.S. Chang ^c

^a Korea Basic Science Institute, 52, Yoeun-dong, Yusong-Ku, Taejon, South Korea

^b Princeton University Plasma Physics Laboratory, Princeton NJ, USA

^c Department of Physics, Korea Advanced Institute of Science and Technology, 373-1 Kusong-dong, Yusong-ku, Taejon, South Korea

Received 5 October 1998; accepted 10 November 1998

Abstract

We present the results of fast time scale plasma control simulations for the proposed Korea Superconducting Tokamak Advanced Research (KSTAR) tokamak. Here, the fast plasma control includes stabilization of the vertical instability and rapid radial position control. As a simulation tool, we use the tokamak simulation code (TSC). We evaluate the power supply requirements for both the vertical and radial position control with a similar approach to that which was employed in the analysis of the tokamak physics experiments (TPX). In particular, we investigate the efficacy of control coil locations to minimize the power supply requirements. From this study, it is shown that two separate sets of control coils, one responsible for vertical control and the other responsible for radial control, are required to provide robust control of both vertical and radial position for all the anticipated plasmas in KSTAR experiments. © 1999 Elsevier Science S.A. All rights reserved.

Keywords: Plasma; Tokamak; Coil locations

1. Introduction

The Korea Superconducting Tokamak Advanced Research (KSTAR) is a proposed experimental device which is intended to develop a steady-state-capable superconduction tokamak to establish the scientific and technological bases for an attractive magnetic fusion reactor [1]. It will

address advanced physics issues such as extension of present stability and performance boundaries of tokamak operation and develop methods to achieve steady state operation of tokamak fusion reactors using non-inductive current drive [1]. Major parameters of KSTAR are shown in Table 1. In order to accomplish the mission and research objectives of KSTAR, it is necessary to possess strong control capabilities. Among the various control issues, control of fast plasma motion is of fundamental importance. Here, ‘fast

* Corresponding author. Tel.: + 82-42-8653618; fax: 82-42-8653619; e-mail: hgijhang@kstar.kbsi.re.kr.

Table 1

The nominal parameters of the Korea Superconducting Tokamak Advanced Research (KSTAR) tokamak

Plasma current (I_p)	2 (MA)
Major radius (R_0)	1.8 (m)
Minor radius (a)	0.5 (m)
Elongation (κ_x)	2.0
Triangularity (δ_x)	0.8
Toroidal field (B_0)	3.5 (T)

plasma motion' mean rapid plasma movements occurring in ~ 10 ms time-scale, which is much faster than the transport time scale. In this paper, we concentrate on this fast time scale control issue for KSTAR

Control of fast plasma motions can be divided into two areas: control of the vertical instability and control of the rapid radial motion. It is well known that vertically elongated tokamak plasmas are inherently unstable to the axisymmetric ($n = 0$) mode (vertical instability) [2,3]. Because nominal KSTAR experiments are designed for high elongation and triangularity ($\kappa_x = 2.0$, $\delta_x = 0.8$), the vertical instability and stabilization of it are of major importance. The vertical instability is an ideal MHD mode and fundamentally involves axisymmetric rigid vertical motion of the entire plasma ($n/m = 0/1$) although higher order non-rigid motion ($n/m = 0/2, 3, \dots$), caused by deformability of plasmas, can lead to more unstable plasmas than rigid analysis would predict [4]. The linear growth rate of this mode depends primarily on the geometry of surrounding conducting structures, the plasma shape parameters such as elongation (κ) and triangularity (δ) and the equilibrium conditions such as plasma beta and internal inductance. Since the growth time of the vertical instability for typical modern tokamak experiments is determined by the poloidal Alfvén time scale ($\sim 10 \mu\text{s}$), a conducting structure must be located close enough to the plasma to slow the plasma motion down by the radial magnetic field induced by the eddy currents. Then, an active control system must be incorporated to compensate for the resistive decay of the passive structure currents and allow us to maintain the plasma at a reference vertical position [5,6]. A typical example of passive structure in tokamaks is the vacuum

vessel. However, if the vacuum vessel is distant from the plasma, it may not provide adequate passive stabilization. In such a case, additional passive structure must be placed within the vacuum vessel to reduce the growth rate. Because of space limitations, the passive stabilizers are typically plate structures of finite poloidal extent. The magnetic coupling between the passive structures and the plasma is non-trivial. The growth rate of the vertical instability can be a strong function of the plasma current profile [7].

Once the surrounding passive structures are defined, the feedback control power critically depends on the vertical growth time and control coil locations. The control coil location is important because the distribution of stabilizing radial magnetic field in the plasma region generated by the control coils depends strongly on coil location. Combined with the plasma current profile, $\vec{J}(\vec{r})$, the radial field, \vec{B}_R , exerts a restoring force, $\int_V dV \vec{J}(\vec{r}) \times \vec{B}_R$ on the plasma. In this paper, we discuss the impact of coil locations on the vertical control capability in detail.

A sudden (~ 1 ms) β (= plasma energy/magnetic energy) drop caused by edge localized modes (ELMs) or minor disruptions will result in a rapid radial shift of the plasma toward the inboard side as a new equilibrium location is established. In order to prevent the plasma from hitting the plasma facing components (PFCs) and to maintain the power coupling between the ICRF antenna and the plasma, an active control system for rapid radial position control is essential.

External copper poloidal field coils (PF coils) can be used as an active control system. However, since the PF coils in KSTAR will be superconducting, they can not respond on such a fast (~ 1 ms) time scale. Thus, internal copper control coils (IC coils) are required inside the vacuum vessel for fast time scale response.

In the present work, we report the results of control simulations of fast plasma motions for KSTAR. As a simulation tool, we use the tokamak simulation code (TSC) [8] throughout the paper. In Section 2, we compute the linear growth time of vertical instability as a function of plasma internal inductance to offer a baseline plasma

condition for the vertical control simulations. In Section 3, we discuss the control of vertical motions in KSTAR. First, we discuss the impact of control coil locations on the control capability. Then, we discuss the process for obtaining optimized feedback system gains from step response simulations. Finally, we evaluate power supply requirements to stabilize random fluctuations of the magnetic axis location [9]. In Section 4, we discuss the control of rapid radial motion. We calculate the maximum coil current and voltage which satisfy the KSTAR design requirements for the radial control system. A summary and some discussions are given in Section 5.

2. Vertical stability for Korea Superconducting Tokamak Advanced Research

In this section, we calculate the linear growth time of the vertical instability for nominal KSTAR plasmas. The plasma vertical growth time depends on the geometry and resistivity of the conducting structure, the plasma current profile $I_i(3)$ and the pressure (β_p). The purpose of the growth time calculations is to identify the $I_i(3)$ and β_p corresponding to the most unstable plasma and present a baseline for vertical control simulation.

Fig. 1 shows the locations of external PF coils, passive structures and internal control (IC) coils being used in the calculation of linear vertical growth time and fast time scale control simulations for KSTAR. The passive structures of KSTAR consist of a double-walled vacuum vessel and an outboard passive stabilizer. The passive stabilizer is made of GLIDCOP and comprises a pair of up-down symmetric plates electrically connected in a saddle configuration with a single toroidal break. This saddle connection is necessary to decouple the passive plates from the ohmic heating system during start up. In order to take this 3-dimensional geometry into consideration for two dimensional TSC simulation, we use an axisymmetric equivalent model derived from the 3-dimensional SPARK code [10]. The SPARK code is used to determine an axisymmetric equivalent geometry and resistance of the passive plates

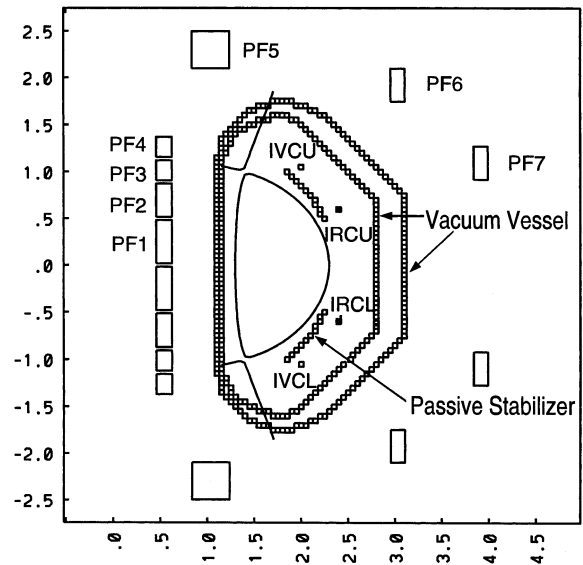


Fig. 1. Axisymmetric structure model of KSTAR used in TSC simulations. The passive structures include double-walled vacuum vessel and the passive plates, which are up-down symmetric and connected into saddle configuration. Two sets of internal control coils are denoted by IVC: (2.00 ± 1.05) and IRC: (2.40 ± 0.60) , respectively.

that reproduces the inductive and resistive responses to up-down asymmetric plasma motion. In the SPARK calculation, we take into consideration other electrical effects such as the conduction paths in the passive plate supports. The resulting effective resistivity of the passive plates is found to be $4.36 \times 10^{-8} \Omega \text{ m}$ although that of pure GLIDCOP is $2.6 \times 10^{-8} \Omega \text{ m}$. We assume that the thickness of passive plates is 0.025 m. The double-walled vacuum vessel of KSTAR is made of stainless steel (resistivity = $180.0 \times 10^{-8} \Omega \text{ m}$) and assumed to be 0.02 m thick. We include the KSTAR vacuum vessel in the TSC calculations.

Once the surrounding passive structures are defined, the vertical growth time depends on the plasma shape, pressure and current profile. We examine the vertical stability for $\beta_p = 0.1$ and $0.6 \leq I_i(3) \leq 1.4$ with other major plasma parameters given in Table 1. Here, $I_i(3)$ and β_p are defined:

$$I_i(3) \equiv \frac{2}{\mu_0 I_p^2 R_0} \int_V B_p^2 dV,$$

$$\beta_p \equiv \frac{4\pi^2 a^2 \langle p \rangle (1 + \kappa^2)}{\mu_0 I_p^2},$$

where I_p is the plasma current and R_0 is the major radius, a is the minor radius, κ is the elongation and $\langle p \rangle$ is the volume averaged plasma pressure, $\langle p \rangle = \int_V p dV/V$. These plasma conditions correspond to expected conditions at the start of current flat top (SOFT), which is characterized by full plasma current, full shape, and ohmic β . These low β SOFT plasmas are expected to be the most unstable ones for the axisymmetric mode during the current flat top stage. For the growth time calculations, we do not include the interactions between the plasma and PF and active control coils.

TSC solves the full nonlinear time dependent resistive magnetohydrodynamic equations [8]. It can accurately model the interactions between the plasma and surrounding conducting structures including passive plates and active control coils.

A reference double null equilibrium is calculated using up-down symmetric coil currents in the seven PF coils external to the vacuum vessel. The equilibrium is then given a small displacement (<1 cm) by introducing antisymmetric coil currents in the internal control coils, IVC upper (U) and IVC lower (L). For the time dependent vertical stability calculations, the coil currents in PF 1–7 are maintained constant in time, however, the control coil currents are made to decay to zero in a very short time period (~ 1 μ s) by giving them an artificially large resistivity. In this way, the double null plasma is perturbed from its equilibrium field location, and a vertical instability is induced.

Fig. 2 shows a typical time history of the last closed flux surface (LCFS) and magnetic axis evolution during a vertical instability. The plasma drifts vertically and eventually shows an exponential dependence of Z_{mag} with time. In this linear phase when $Z_{\text{mag}} \sim \exp(-t/\tau_z)$, the growth time, τ_z , is independent of time.

Fig. 3 shows the vertical growth time as a function of $I_i(3)$ for $\beta_p = 0.1$ and nominal KSTAR plasma parameters given in Table 1.

Note that the plasma is most unstable when $I_i(3)$ is either small or large (i.e. for both hollow and peaked current profiles). The tendency that the vertical growth time is reduced for small $I_i(3)$ has been reported also in [7]. A possible explanation for this phenomenon in terms of passive stabilizer location will be given in the next section. For high $I_i(3)$, the increase of effective distance between the plasma current centroid and the passive stabilizer leads to degradation of vertical stability. However, the degradation at low $I_i(3)$ is more severe than high $I_i(3)$ in the case considered.

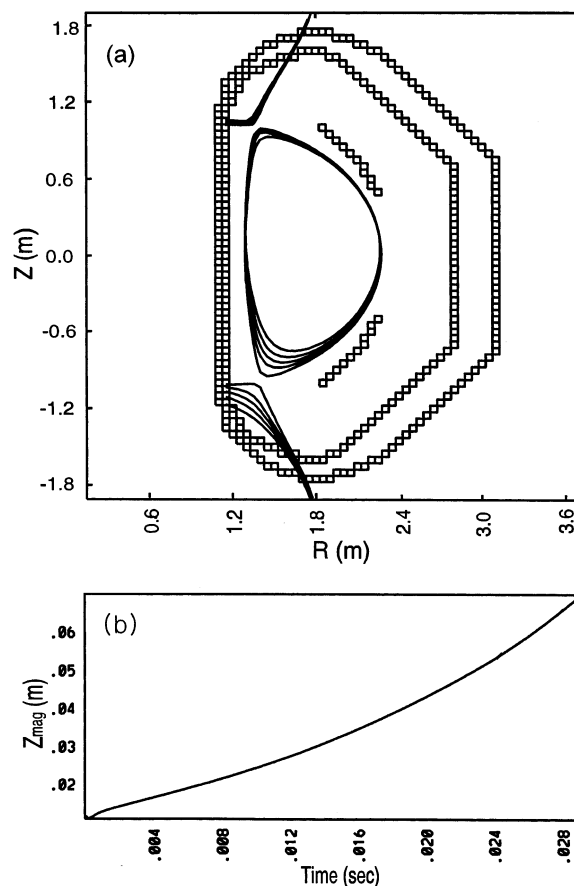


Fig. 2. Time evolutions of (a) last closed flux surface (LCFS) AND (b) magnetic axis in vertical direction (Z_{mag}) during a vertical growth time calculation. The plasma conditions are $\beta_p = 0.1$, $I_i(3) = 1.4$ with plasma parameters given in Table 1.

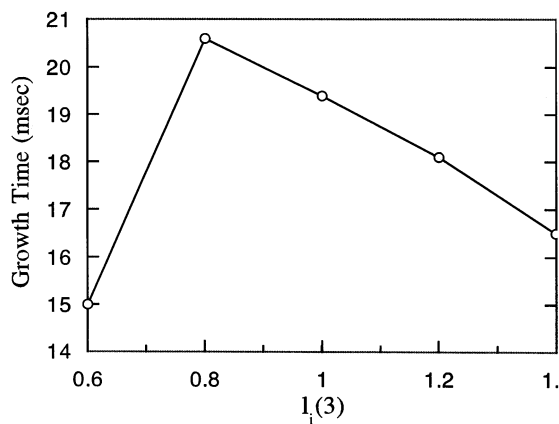


Fig. 3. Growth time of the vertical instability as a function of $I_i(3)$. The same plasma parameters as in Fig. 2 except for $I_i(3)$ have been used.

3. Control of vertical instability

3.1. Impact of control coil locations on control capability

The main factors that determine the power supply requirements for control coils are the vertical growth time and the locations of control coils. The more unstable the plasma is, the larger is the required control power.

The control coil location is important because the strength and distribution of stabilizing radial magnetic field in the plasma region generated by the control coils depends strongly on coil location. The total restoring force exerted on the plasma is a function of the plasma current profile and the distribution of the stabilizing radial magnetic field generated by the control coils, hence the control coil location.

A simple physical mechanism for the impact of control coil locations on the control capability can be delineated from Fig. 4. Suppose that a pair of control coils is located between the midplane and top of the plasma (such as IRC in Fig. 1). If the plasma is perturbed above the midplane, the upper control coil will provide coil current that flows in the opposite direction to the plasma current to stabilize the unstable vertical plasma motion. This coil current exerts a downward stabilizing force on that part of the plasma which is below the control coil. However, there is a portion of the plasma

which is above the control coil. As a result, the coil current stabilizes a part of the plasma while it also destabilizes the other part. The net effect is the reduction of restoring vertical force produced by the coil current. See Fig. 4(a).

An equivalent statement can be given in terms of the distribution of the radial magnetic fields in the plasma region produced by the control coil currents. The sign of radial magnetic field, which is responsible for stabilization, will change in the vicinity of the coil locations. Hence, the total restoring force given by:

$$\vec{F}_z = \int_V \vec{J}(\vec{r}) \times \vec{B}_R(\vec{r}) dV,$$

where $\vec{J}(\vec{r})$ is the plasma current density profile and $\vec{B}_R(\vec{r})$ is the radial magnetic fields produced by the coil currents, will also change. The net effect is the reduction of total restoring force due to the smallness of the strength of the radial magnetic field and sign change of the restoring force in the vicinity of the control coil locations. The reduction of total restoring force becomes more severe when the plasma current profile is very broad or even hollow. It is not hard to see that if the coils are located at $Z \geq Z_{\text{top}}$, there is an advantage for a broad or hollow current profiles while it is unfavorable for a peaked one due to the smallness of B_R at the plasma center. Fig. 4(b) shows the absolute value of normalized radial magnetic fields inside the plasma at the major radius generated by the IVC and IRC in Fig. 1. The (R, Z) locations of IVC are fixed at (2.00 ± 1.05) and (2.40 ± 0.60) , respectively. The radial magnetic field generated by IRC is larger and has the same sign for all the plasma region while that using IVC is small and changes its sign in the vicinity of the coil location.

If we use IVC as vertical control coils, the worst case plasma to control will be the one with high $I_i(3)$ while that of IRC will be the one with low $I_i(3)$. Determination of vertical control coil location requires detailed calculation of power consumption to stabilize the vertical instability of the baseline plasmas for each coil set. In the present work, we have found that it is more efficient to use IVC for vertical control. This will be described in the next subsection in greater detail. We will use $I_i(3) = 1.4$ as the baseline plasma although

the growth time for $l_i(3) = 1.4$ is somewhat larger than that of $l_i(3) = 0.6$ (see Fig. 3). Our choice of the baseline plasma for the IVC will also be justified quantitatively in the next subsection.

Another important point for determining the efficient placement of control coils is the coupling between the control coils and passive stabilizer. We must minimize the mutual inductance between the passive stabilizer and the control coils because of the shielding of the active coil currents by the stabilizer. In this sense, it would be advantageous to place the coils on the inboard side of the

plasma [11,12]. In KSTAR, however, there is insufficient space on the inboard side to accommodate the control coils. Hence, their placement on the outboard side. The shielding of IVC by the passive plates is found to be tolerable.

A similar analysis can be applied to interpret the degradation of vertical stability for low $l_i(3)$. Because a great portion of the passive plates for the present KSTAR design lies below the top of the plasma (Fig. 1), the stabilizing effect of the passive plates for very broad or hollow current profiles is somewhat reduced compared with that

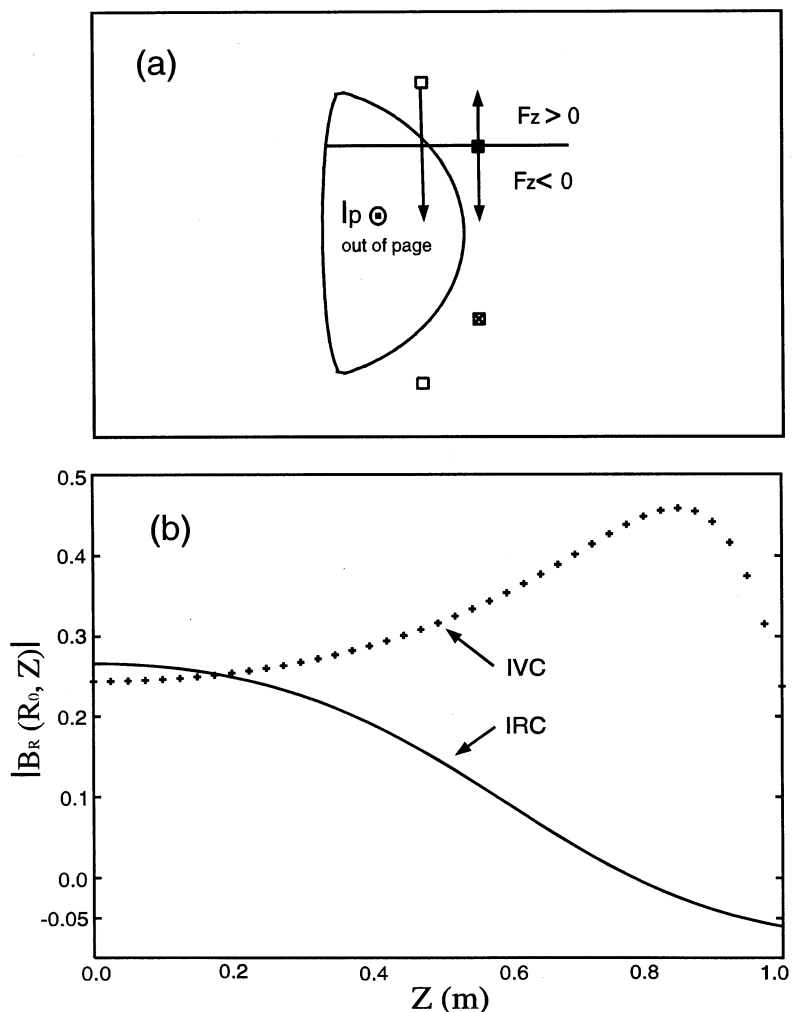


Fig. 4. (a) Impact of control coil locations on control capability and (b) absolute value of normalized radial magnetic fields generated by IVC (cross line) and IRC (solid line) as a function of Z at $R = R_0$.

for peaked current profile. This will lead to the degradation of vertical stability for low $I_i(3)$. We have found that the growth time increases with decreasing $I_i(3)$ if the entire passive plate is located above the top of the plasma. However, the degradation of vertical stability for high $I_i(3)$ in the latter case was much more severe than that for $I_i(3)$ in the present KSTAR stabilizer geometry because of the large increase of effective distance between the plasma current centroid and the passive plates. However, the degradation of the vertical stability for low $I_i(3)$ in the present KSTAR passive plates is tolerable.

3.2. Step response simulation

In this subsection, we describe step response simulations where the control coils are required to provide a 2 cm shift in vertical position. We assume that a 2 cm shift represents the maximum likely step perturbation in KSTAR. The step response simulations provide a simple and direct way of examining the feedback characteristics of the control system. The simulations determine the optimum feedback system gains which minimize power supply consumption.

The present design requirements of the KSTAR vertical feedback control system are that it provides a 2 cm offset in vertical position and that it stabilizes a random disturbance characterized by $\Delta Z_{\text{rms}} = 1$ cm with a power spectral bandwidth $\Delta\omega = 1/\tau_z$, where τ_z is the plasma growth time, for all the anticipated plasmas in KSTAR experiments [1]. The random simulation will be described in the next section. We use the IVC control coils shown in Fig. 1 as vertical control coils. As a baseline plasma, we choose a plasma with $I_i(3) = 1.4$ and $\beta_p = 0.1$, the same conditions given in Section 2. Such a plasma will require the largest power consumption among all the expected plasmas.

For the feedback system control law, we use proportional and derivative (PD) gain control given by:

$$I_f = g_p (Z_{\text{mag}} - Z_0) + g_d \frac{d}{dt} (Z_{\text{mag}} - Z_0) \quad (1)$$

where Z_{mag} represents the vertical position of the plasma magnetic axis, Z_0 is the desired value of Z_{mag} (in this case $Z_0 = 2.0$ cm), g_p and g_d are the proportional and derivative gains, respectively. Here, it is assumed that the vertical position of the plasma magnetic axis can be measured and used for vertical feedback.

Fig. 5 shows the time evolutions of Z_{mag} and the IVC coil currents for the baseline plasma during a step response simulation. The proportional gain in Eq. (1) is responsible for the active coil currents holding the plasma at 2 cm above the midplane. If g_p is too small, the control coils can not hold the plasma at the desired point and if g_p is too large, the feedback system requires more current than is necessary. The optimal g_p is determined from a sequence of simulations where the gain is varied. Once the optimal g_p is found, we determine a value for the derivative gain, g_d in Eq. (1). It is well known that g_d affects the reaction time of the feedback system and the inclusion of a derivative gain term reduces the power supply consumption of the control coils [11]. The procedure to select the optimized g_d can be explained using Fig. 5(b) and Fig. 6. In order to obtain a 2 cm shift in Z_{mag} , the plasma must initially be pulled by the IVCU and pushed by the IVCL. This results in a positive current in IVCU and a negative current in IVCL at early times (the direction of plasma current is positive). As the plasma moves vertically, the coil currents must change their signs to prevent overshoot of the plasma beyond the desired 2 cm offset. Thus, there exists a time at which $dI_f/dt|_{t=t_0} = 0$ and the feedback currents at this time point are determined by the size of the derivative gain. If g_d is too small for a given g_p , the feedback system can not respond quickly enough to the plasma motion and the initial coil current spike has a maximum value that is larger than the steady state value, although Z_{mag} reaches the desired reference more quickly [see Fig. 6(a) and (b)]. If g_d is too large, the initial current spike is smaller than the steady state value but the system is sluggish [see Fig. 6(c)]. In this case, there is no reduction of power supply currents because the steady state currents are the same regardless of the g_d . Hence, we can regard this large g_d as the worst choice of the derivative

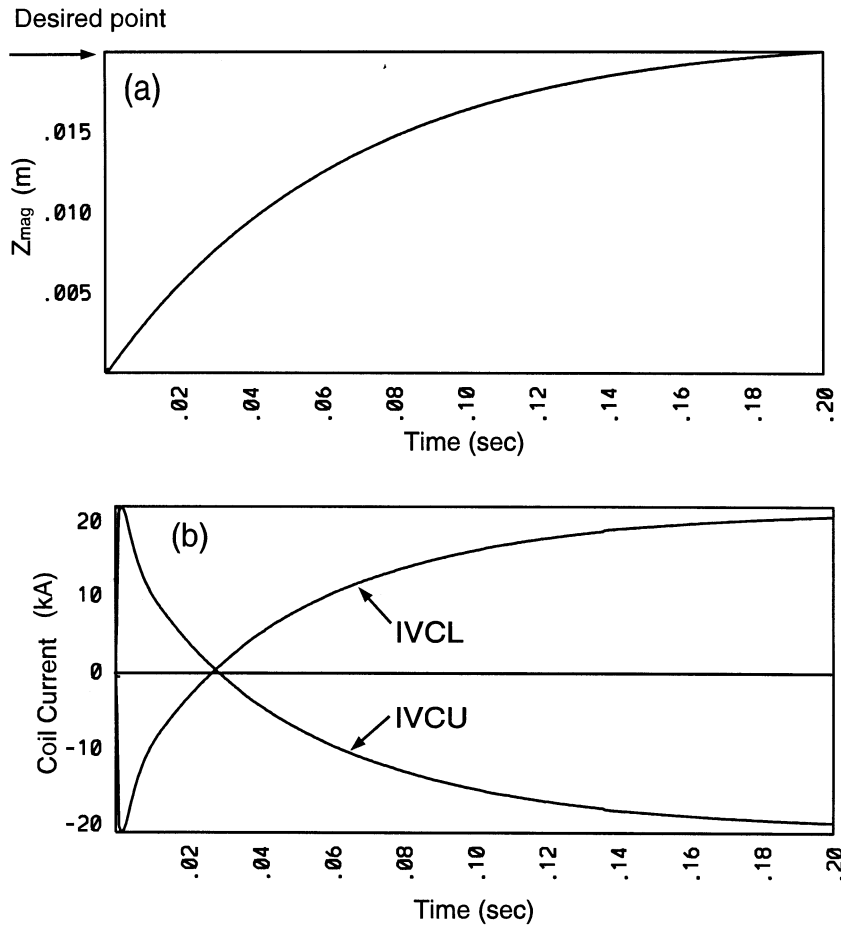


Fig. 5. Time histories of (a) plasma vertical position and (b) control coil currents during a step response simulation. We have used IVC as vertical control coils. The plasma parameters are the same as those of Fig. 2.

gain. The optimization of the vertical feedback system gains is achieved by choosing a g_d that gives the same initial magnitude for the current spike as the steady state current value. The result of such a procedure is shown in Fig. 5. These criteria generally leads to Z_{mag} trajectories that are slightly overdamped in the step response. However, we have found that the responses in the random disturbance simulations are not affected significantly by this choice of derivative gain.

In real experiments, the feedback gains are fixed during the discharges and we may use the optimized gains chosen from the plasma with $l_i(3) = 1.4$ (Fig. 5) since it corresponds to a worst

case scenario. We expect that the feedback powers for all the anticipated plasmas will be lower than for this baseline case. Fig. 7(a) shows the maximum current for different values of $l_i(3)$ for step response simulations. We use the optimized gains found in Fig. 5. As expected, the maximum currents for all the $l_i(3)$ cases examined are lower than for $l_i(3) = 1.4$. This justifies our choice of the baseline plasma. Note that the maximum current for $l_i(3) = 0.6$ is slightly smaller than for $l_i(3) = 1.4$ even though the plasma with $l_i(3) = 0.6$ is somewhat more unstable (Fig. 3). The reason is that the location of IVC is more favorable for stabilizing low $l_i(3)$ plasmas, as was discussed in the last subsection.

In order to investigate the effects of coil locations in more detail, we have performed the step response simulations using the IRC in Fig. 1. In this case, the baseline plasma is chosen as $I_i(3) = 0.6$ on the basis of the discussions presented in the last subsection. The same procedures were used for analyzing control using IRC as were used for the analysis of IVC. Fig. 7(b) shows the maximum

IRC current as a function of $I_i(3)$. It is obvious from Fig. 7 that the low $I_i(3)$ is indeed the worst case for vertical control and the power supply requirements for IRC are greater than those of IVC for the entire range of $I_i(3)$. Thus, it is concluded that the IVC are more efficient than the IRC for vertical control of all the plasmas anticipated in KSTAR discharges.

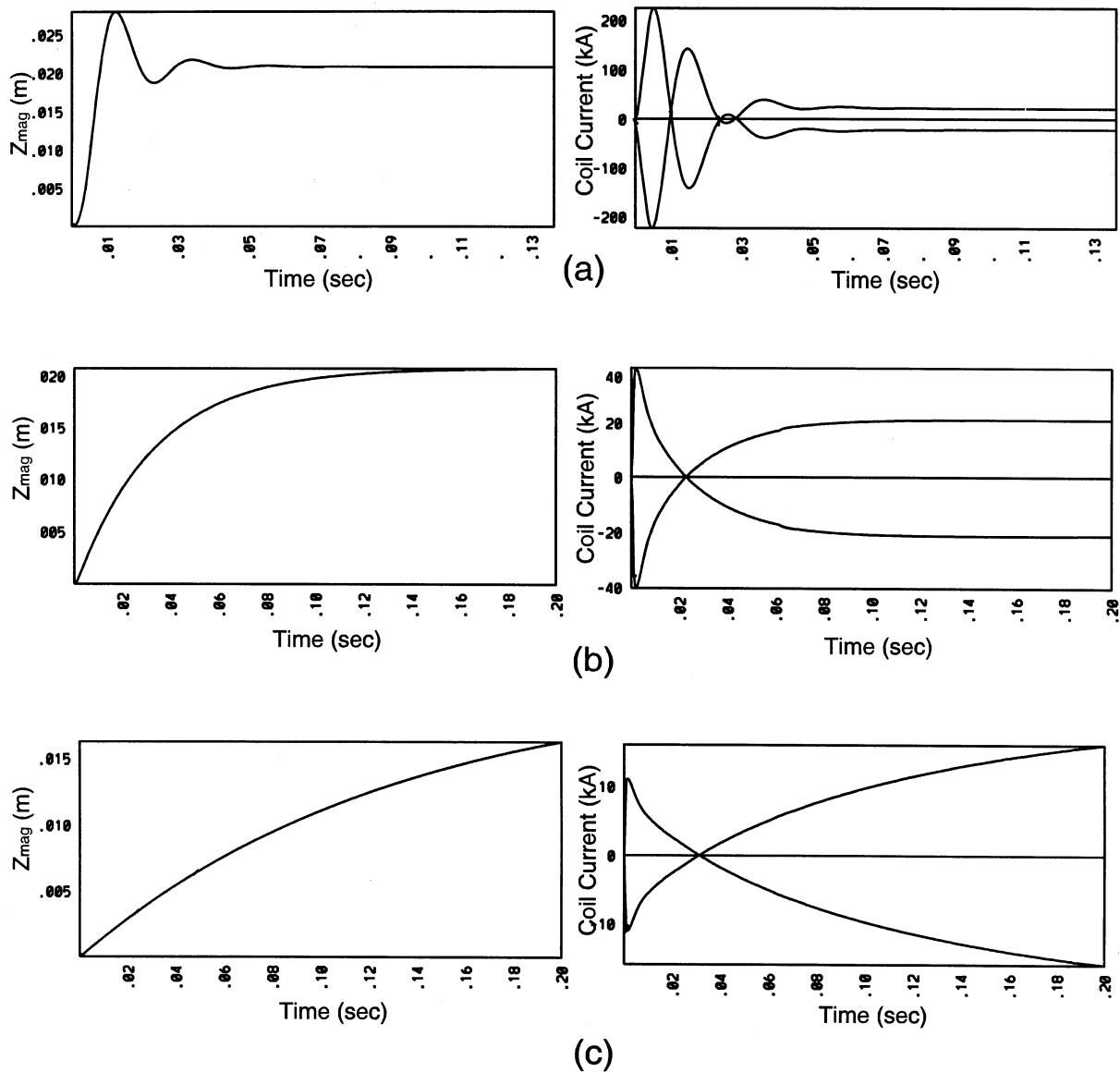


Fig. 6. Plasma vertical position and coil currents as functions of time in step response simulations with not optimized derivative gains: (a) $g_d = 0.01g_d^{opt}$; (b) $g_d = 0.5g_d^{opt}$; and (c) $g_d = 2g_d^{opt}$. Here, we use the same g_p and g_d^{opt} , which are determined from Fig. 5. We have used IVC as vertical control coils.

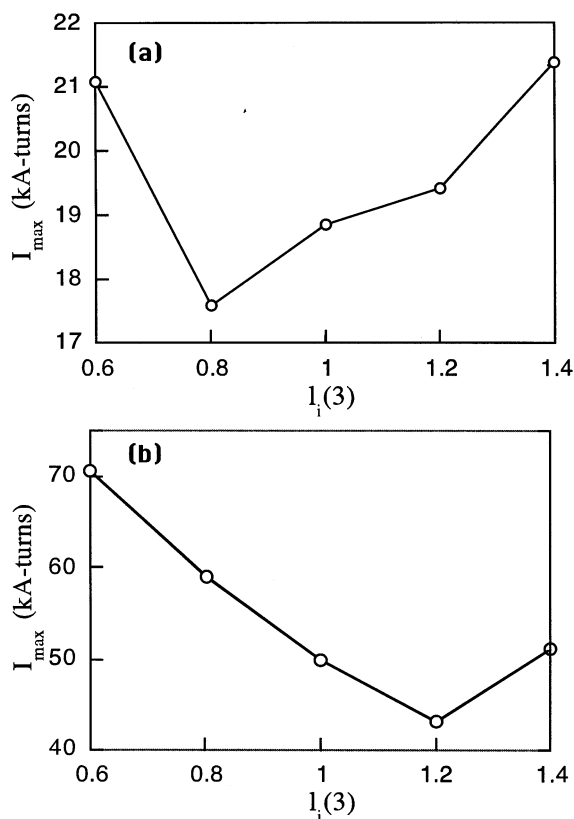


Fig. 7. Maximum current in the step response simulations as a function of $I_i(3)$ for (a) IVC and (b) IRC. Note that $I_i(3) = 1.4$ gives rise to maximum current for IVC while $I_i(3) = 0.6$ does for IRC.

3.3. Random disturbance simulation

After the gains for the vertical feedback system have been optimized from the step response simulation, we calculate the maximum coil currents and voltages (i.e. the power supply requirements for the control coils) from a random disturbance simulation [9]. The random disturbance is simulated by feeding the control coils a random signal to move the plasma from position to position. The random disturbance in magnetic axis is given by:

$$Z_0(t) = 2Z_0 \left[\frac{\pi\tau}{T} \right]^{1/2} \sum_{n=1}^{\infty} \exp\left(-\frac{\omega_n^2 T_n^2}{8}\right) \times \cos(\omega_n t - \phi_n), \quad (2)$$

where Z_0 is the amplitude, τ is the autocorrelation time and T is the period of the random disturbance. Also, $\omega_n = 2n\pi/T$ and ϕ_n is a uniform random phase ($-\pi \leq \phi_n \leq \pi$). The root-mean-square disturbance of Z_{mag} is fixed to be 1 cm. The choice of this level of disturbance is motivated by experimental results observed on JET, DIII-D and PBX-M. The source for the random disturbance can be field perturbations and/or measurement errors. The autocorrelation time τ in Eq. (2) is related to the power spectral bandwidth by $\tau = \sqrt{\pi/\Delta\omega}$, with $\Delta\omega = 1/\tau_z$, where τ_z is the plasma growth time for the baseline plasma (16.5 ms). Also, we include a 1.0 ms time delay for the control system to represent measurement processing and power supply activation.

Fig. 8 represents the time histories of plasma vertical position and coil currents and voltages during a random disturbance simulation. We do not limit the power supply voltage. The maximum excursion of Z_{mag} is about 2 cm. The maximum current and voltage are found to be 93 kA-turns and 63 V turn⁻¹, respectively. These are about two times larger than those determined in the TPX design studies [9], which were 45 kA-turns and 25 V turn⁻¹, respectively. The primary reason for this is due to the smaller vertical growth times for baseline KSTAR plasmas (16.5 ms) compared with TPX plasmas (40.0 ms). KSTAR plasmas have a smaller growth time than TPX due to the lack of inboard passive plates and a larger plasma to passive plate distance on the outboard.

It is interesting to compare the maximum currents and voltages using the IRCs for vertical control with those obtained above using the IVCs. The same random disturbance simulation using an $I_i(3) = 0.6$ baseline plasma leads to maximum current and voltages of 155 kA-turns and 138 V turn⁻¹, respectively, which are much larger than those obtained using the IVC. Thus, it is confirmed that we can minimize the control power consumption if we use IVC rather than IRC as vertical control coils.

4. Rapid radial position control

A sudden drop of the plasma internal energy causes a loss of radial force balance and hence, a rapid inward radial motion of the entire plasma column as it seeks a new magnetohydrodynamic

equilibrium at the reduced pressure. The principal goals of rapid radial position control are to maintain good coupling between the RF and lower hybrid wave launchers and the plasma, and to protect the plasma facing components. In principle, the IVC or IRC might be used to control the

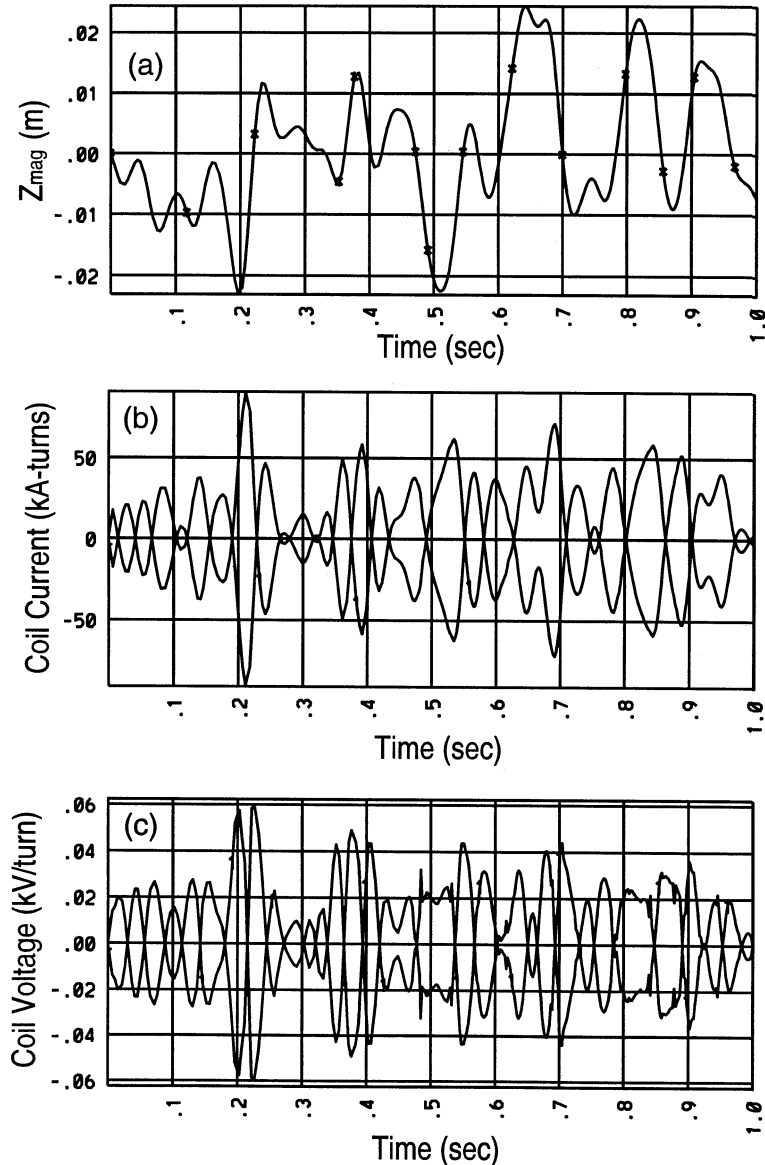


Fig. 8. Time histories of (a) plasma vertical position (b) coil currents and (c) voltages during a random disturbance simulation. We have used IVC as vertical control coils. The plasma parameters are the same as those of Fig. 5. The random signal is characterized by $\Delta Z_{\text{rms}} = 0.01$ m. The maximum current and voltage are found to be 93 kA-turns and 63 V turn^{-1} , respectively.

radial position. However, we find that the IVC is inappropriate for this use. The shielding of coil currents by the passive plates is minimal for radial control because the plates are connected in a saddle configuration with a resistive connector to the vacuum vessel. As a consequence, the up–down symmetric eddy currents induced by the radial plasma motion and control coil currents decay extremely rapidly due to a $600 \mu\Omega$ gap resistance for up–down symmetric currents in each passive plate.

In terms of antenna-plasma coupling, it is natural to choose the outboard plasma major radius as the control variable. Thus, we use a feedback system law given by:

$$I_f = g_p [(R_0 + a) - (R_0 + a)_{\text{ref}}] \quad (3)$$

Here, $(R_0 + a)_{\text{ref}}$ is the desired radial position, which is equal to 2.3 m for KSTAR. We have found that using only the proportional gain is sufficient to control the rapid radial motion.

It is clear that the worst case plasma for radial control is the highest β plasma, since such a plasma allows the largest possible β drop. As a baseline plasma for radial control simulations, we choose a plasma with the normalized beta, $\beta_N = 5.0$, where $\beta_N \equiv \beta_T (\%) / (I (MA) / a (m) B_T (T))$, $l_i(3) = 0.8$ and the plasma parameters given in Table 1. The $\beta_N = 5.0$ is the largest β_N expected to be achieved in KSTAR. As a model disturbance for evaluating the feedback system requirements, we use an edge localized mode (ELM)-like oscillation, which exhibits a sudden β drop within ~ 1 ms and recovers to its full value on an energy confinement time scale. The design requirement is to provide control of $(R_0 + a)$ within 25 ms (i.e. bring the outboard plasma major radius back its original position within 25 ms) for 20% ELM-like beta drops every 100 ms with recovery.

Figs. 9 and 10 represent the time histories of the plasma internal energy, control coil current and voltage, outboard $(R_0 + a)$ and inboard $(R_0 - a)$ plasma major radii. Here, we use the IRC as radial control coils. In the simulation, as in the vertical control simulations, we do not restrict the power supply voltage. The plasma

internal energy is preprogrammed to drop every 100 ms and to recover its original value to immediately prior to the next drop. The maximum coil current and voltage are found to be 56 kA-turns and 117 V turn⁻¹, respectively. The outboard plasma major radius is brought back to within 1 cm of its original position about 25 ms after the radial control system is turned on, as is shown in Fig. 10(a). The inboard major radius decreases somewhat with time because the plasma is deformed by the feedback current, resulting in an increase of minor radius.

The efficiency of different control coil locations on the radial control capability can be shown in Fig. 11. Fig. 11(a) shows the vertical magnetic fields inside the plasma at the geometric center, R_0 , as a function of Z and Fig. 11(b) represents the vertical magnetic fields inside the plasma on the midplane as a function of R , generated by the IVC and IRC. As we can see in Fig. 11, the magnitude of vertical fields inside the plasma generated by the IRC are much larger than those generated by the IVC in all the plasma region. We see that the IRC is much more effective than the IVC for radial control. We have found that the impact of coil locations on the radial position control is more significant than for vertical control. Using IVC as radial control coils, we can not find any gain to satisfy the desired design requirement. Remember that we can still stabilize the vertical plasma motion using IRC although the power consumption is about two times larger than that of IVC. Thus, it is concluded that we can only use the IRC to control the rapid radial motion.

5. Summary and conclusions

In this paper, we have investigated the fast plasma control issues for proposed KSTAR tokamak plasmas. Throughout the paper, we have used the TSC code as a simulation tool. We have examined the vertical stability for reference KSTAR plasmas including the presently defined conduction structures, passive stabilizer plates and the double-walled vacuum vessel. It has been shown that the plasma is most stable

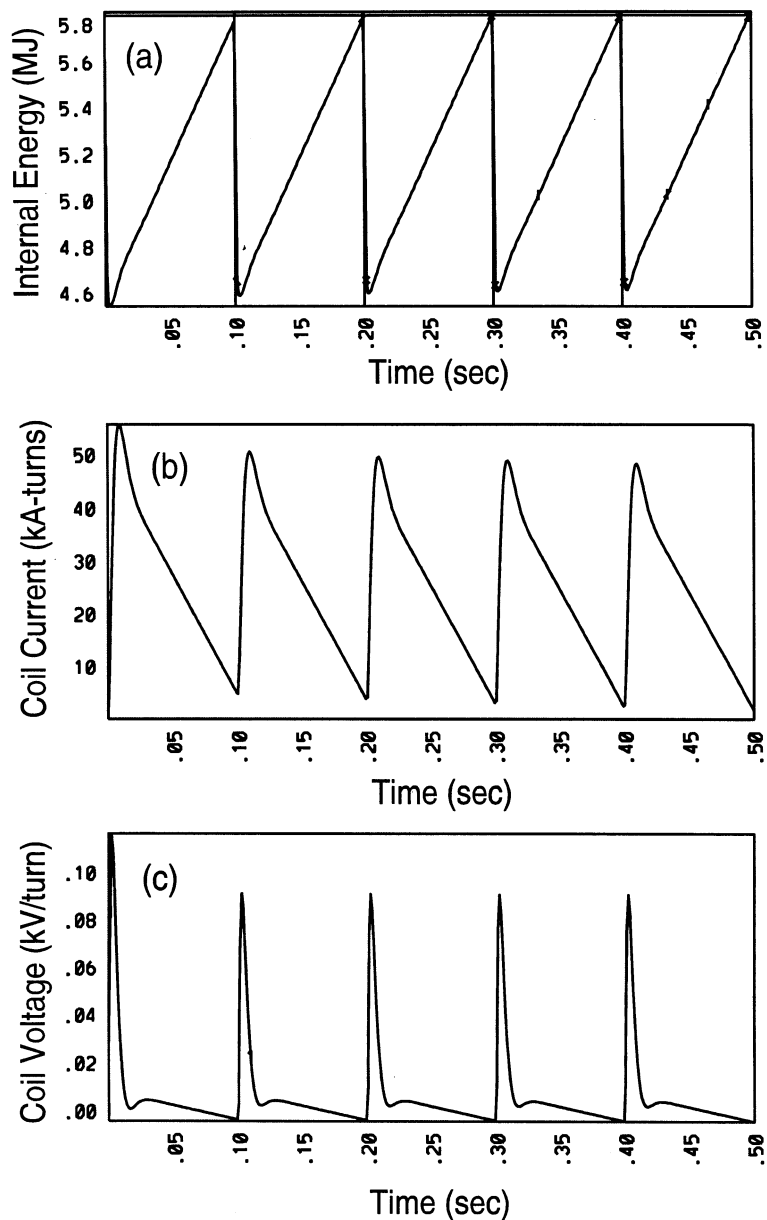


Fig. 9. Time histories of (a) plasma internal energy (b) control coil current and (c) voltage during a radial control simulation. The radial disturbance is modeled as 20% drop in the internal plasma energy every 100 ms. A high β plasma ($\beta_N = 5.0$) with $I_i(3) = 0.8$ and plasma parameters in Table 1 has been used. We use IRC as radial control coils.

near $I_i(3) = 0.8$ and becomes unstable as $I_i(3)$ increases or decreases. The degradation of vertical stability for low and high $I_i(3)$ has been argued on the basis of the geometry of the present passive stabilizer.

The importance of the active control coil locations on the control capability has been investigated. For vertical control, it is found that it is beneficial to use IVC because it minimizes the power supply consumption. The power supply

requirements have been evaluated from random disturbance simulations, which model a 1 cm root-mean-square random disturbance in the detected magnetic axis location during a discharge. Using IVC, the maximum current and voltage to stabilize the random disturbances in the magnetic axis are found to be 93 kA-turns and 63 V turn^{-1} , respectively, which are approximately two times smaller than those obtained using the IRC. For radial control, we have found that only IRC can be used for effective control. The maximum coil current and voltage to satisfy the design requirements have been calculated for ELM-like oscillations, which exhibit a 20% drop of the stored plasma energy in 1 ms every 100 ms. The current and voltage are found to be 56 kA-turns and 117 V turn^{-1} , respectively. One note is that we do not restrict the power supply voltage in the control simulations. If the voltage limit is introduced, the maximum voltages and currents might be different from the present results.

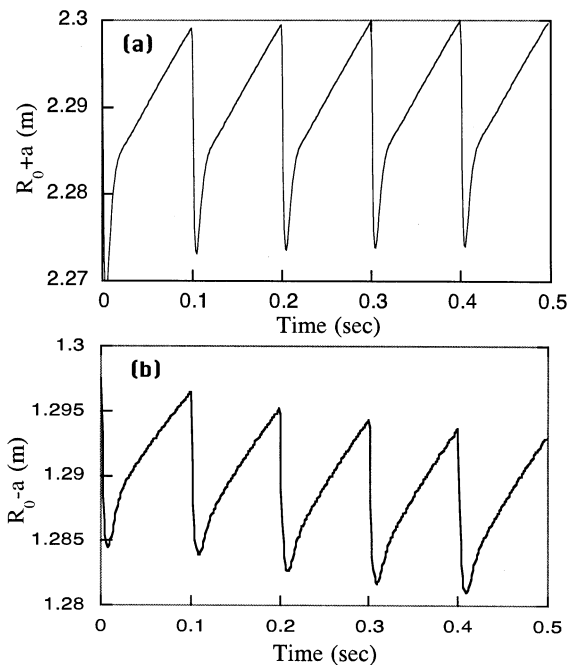


Fig. 10. Time histories of (a) outboard ($R_0 + a$) and (b) inboard ($R_0 - a$) major radii during a radial control simulation described in Fig. 9.

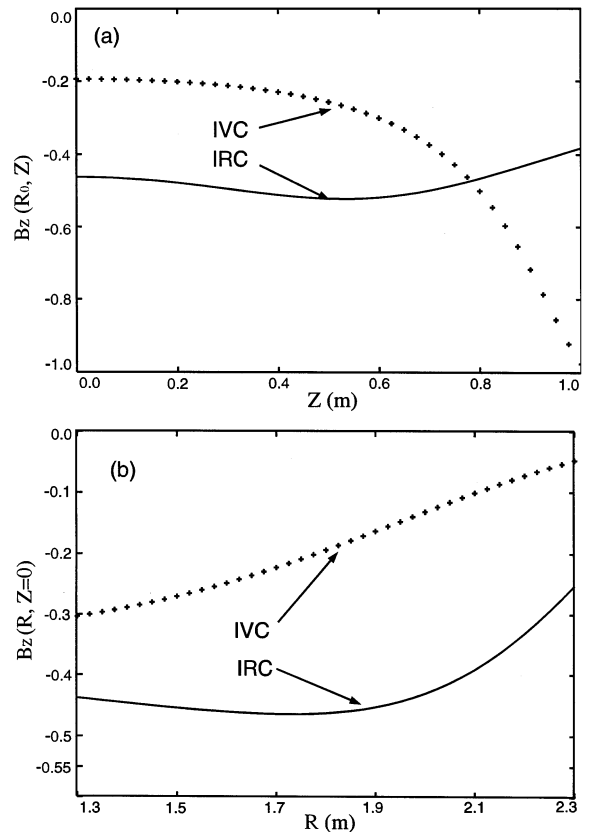


Fig. 11. (a) The normalized vertical magnetic fields generated by IVC (cross) and IRC (solid line) as a function of Z at $R = R_0$. (b) The normalized vertical magnetic fields generated by IVC (cross) and IRC (solid line) as a function of R at $Z = Z_0$.

The main conclusion of the control simulations is that we should use two separate sets of coils to control both the vertical and radial motions with minimized power supply requirements. The analyses adopted in the present work will also be helpful for the design study of other future tokamaks which are intended to employ the fast plasma control system.

Acknowledgements

One of the authors (HJ) wishes to acknowledge helpful discussions with Dr J.Y. Kim of Korea Basic Science Institute and S.H. Ku of Korea Advanced Institute of Science and Tech-

nology. This work was supported by the Korea Ministry of Science and Technology.

References

- [1] D.I. Choi, G.S. Lee, J. Kim, H.K. Park, C.S. Chang et al., The KSTAR Tokamak, in: Proceedings of The Seventeenth IEEE/NPSS Symposium Fusion Engineering vol. 1, San Diego, CA, October 6–10, 1997, pp. 215–220.
- [2] G. Laval, R. Pellat, J.S. Soule, Hydromagnetic stability of a current-carrying pinch with noncircular cross section, *Phys. Fluids* 17 (1974) 835–845.
- [3] V.S. Muchovatov, V.D. Shafranov, Plasma equilibrium in a Tokamak, *Nucl. Fusion* 11 (1971) 605.
- [4] D.J. Ward, S.C. Jardin, C.Z. Cheng, Calculations of axisymmetric stability of Tokamak plasmas with active and passive feedback, *J. Comput. Phys.* 104 (1993) 221–240.
- [5] S.C. Jardin, D.A. Larrabee, Feedback stabilization of rigid axisymmetric modes in Tokamaks, *Nucl. Fusion* 22 (1982) 1095–1098.
- [6] D.J. Ward, F. Hofmann, Active feedback stabilization of axisymmetric modes in highly elongated Tokamak plasmas, *Nucl. Fusion* 34 (1994) 401–415.
- [7] D.J. Ward, A. Bondeson, F. Hofmann, Pressure and inductance effects on the vertical stability of shaped Tokamaks, *Nucl. Fusion* 33 (1993) 821–828.
- [8] S.C. Jardin, N. Pomphrey, J. Delucia, Dynamic modeling of transport and position control of Tokamaks, *J. Comput. Phys.* 66 (1986) 481–507.
- [9] C.E. Kessel, S.C. Jardin, R.H. Bulmer, R.D. Pillsbury, Pei-Wen Wang, G.H. Neilson, D.J. Strickler, Poloidal field control for the Tokamak physics experiment, *Fusion Tech.* 30 (1996) 184–200.
- [10] D. Weissenburger, SPARK Version 1.1: Users Manual, Rep. PPPL-2494, Princeton Plasma Physics Laboratory, NJ, 1988.
- [11] E.A. Lazarus, J.B. Lister, G.H. Neilson, Control of the vertical instability in Tokamaks, *Nucl. Fusion* 30 (1990) 111–141.
- [12] J.B. Lister, Y. Martin, J.M. Moret, On locating the poloidal field coils for Tokamak vertical position control, *Nucl. Fusion* 36 (1996) 1547–1560.